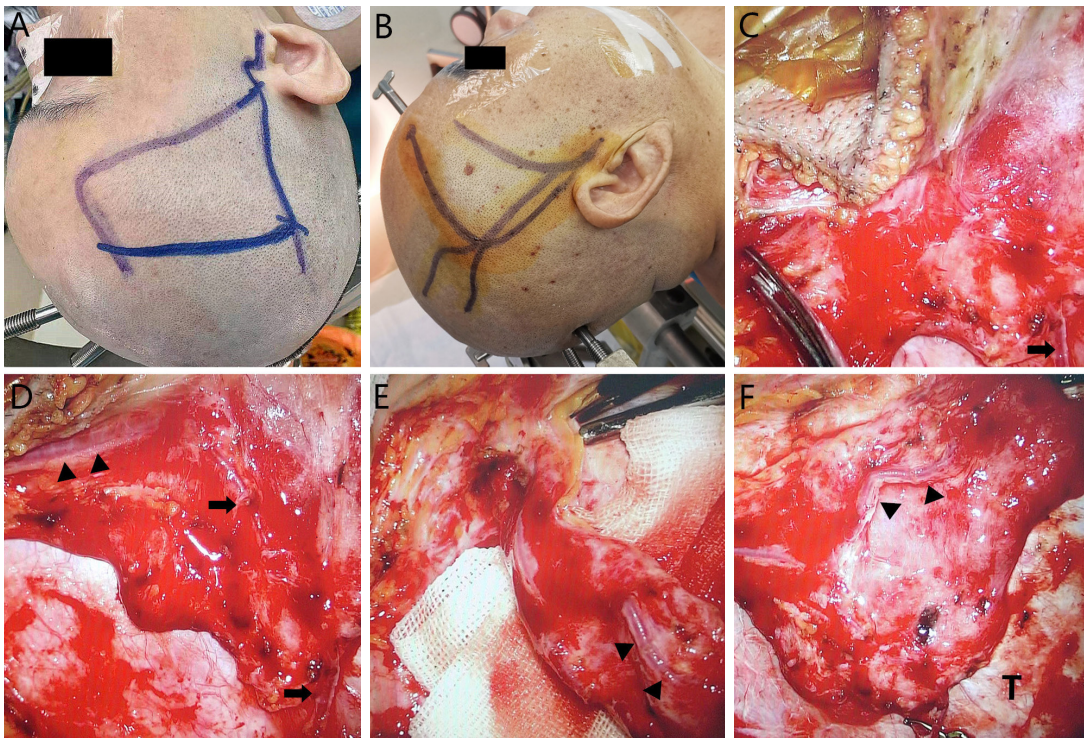

Figure S1 Intraoperative photographs showing the skin incision and step-by-step procedures of the TPFF acquisition. (A) An inverted L-shaped incision was formed by extending along the parietal branch of the STA to the supratemporal line and then curling toward the forehead hairline. (B) A curved incision which shape behind the parietal branch of the STA. (C) The distal end of the STA parietal branch (arrow) below the subcutaneous fat layer was dissociated. (D) The STA trunk (triangles) was separated above the zygomatic arch along the parietal branch of the STA (arrows). Separation was made forward to the distal of the frontal branch of STA around the pterion of the skull. (E) The TPFF was separated along the leading edge of the frontal branch of the STA (arrowhead), and attention was given to avoid facial nerve injury. (F) The Fan-shaped TPFF was completely separated on the temporal myofascial (T) surface, and the frontal branch of the STA (triangles) within the TPFF was intact. These images are published with the patient's consent. TPFF, temporoparietal fascial flap; STA, superficial temporal artery; T, temporal myofascial.

© Annals of Translational Medicine. All rights reserved.
https://dx.doi.org/10.21037/atm-22-5281

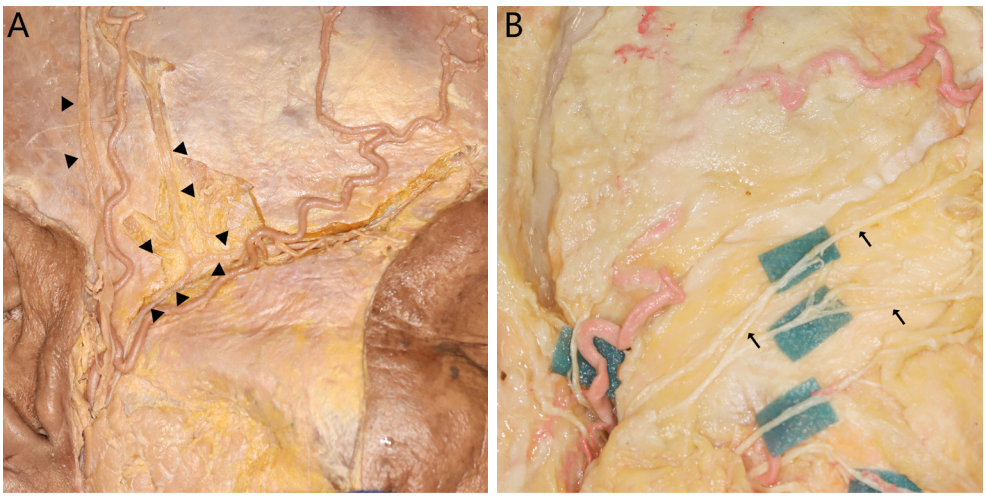

Figure S2 Anatomical photographs show the relationship between STA, STV, and facial nerve. (A) STV (triangles) rises along the posterior edge of the parietal branch of the STA, and the STV receives reflux from the internal branch of TPFF on the upper zygomatic arch. (B) Temporal branch of the facial nerve is shaped in front of the TPFF (arrows). STA, superficial temporal artery; STV, superficial temporal vein; TPFF, temporoparietal fascial flap.

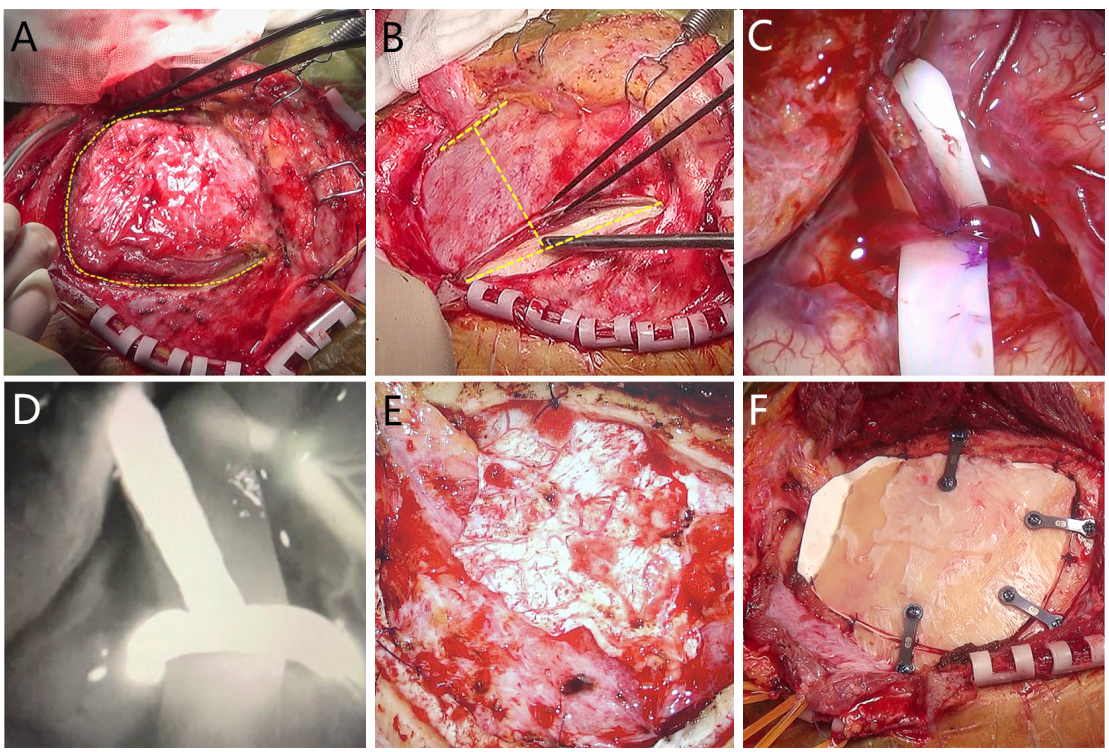

Figure S3 Intraoperative photographs show intraoperative vascular anastomosis and skull opening and closing procedures. (A) The C-type incision for normal temporal muscle (yellow dotted line). (B) The h-type incision for hypertrophic temporal muscle (yellow dotted line). (C) The end-to-side anastomosis was completed without blood leakage at the anastomotic site. (D) Intraoperative fluorescence contrast was used to verify the patency of the anastomotic site. (E) TPFF was loosely sutured to the peripheral dura, and the curved dura flap was located above the TPFF. (F) The bone flap around the root of the TPFF was removed to avoid compression. TPFF, temporoparietal fascial flap.

© Annals of Translational Medicine. All rights reserved.
https://dx.doi.org/10.21037/atm-22-5281

Table S1 Clinical characteristics (n=31)

Variables	Mumeric data
Ischemic MMA	24
Hemorrhagic MMA	7
Female:male	19:12
Admission age, years	
Mean ± SD	40.5±10.6
Range	21–63
Nidus location, n	
Left side	23
Right side	8
Indications for revascularization, n	
TIA	3
Cerebral infarction	21
ICH	2
IVH with ICH	5
Clinical presentation, %	
Limb weakness	68%
Aphasia	48%
Blurred vision	13%
Dizziness	10%
Seizure	3%
Calculation and memory loss	3%
Headache	3%
Asymptom	6%
Suzuki angiographic stage, n	
III	20
IV	11
Time interval between symptom presentation and admission, months	
Mean ± SD	9.4±16.2
Range	1–84
Duration of follow-up, months	
Mean ± SD	21.1±10.3
Range	6–38

MMA, moyamoya angiopathy; TIA, transient ischemic attack; ICH, intracranial hemorrhage; IVH, intraventricular hemorrhage.

© Annals of Translational Medicine. All rights reserved.
https://dx.doi.org/10.21037/atm-22-5281

Table S2 Outcomes and complications

Variables	Mumeric data
mRS score, n=31	
Admission, mean	1.00; ref.
One month after surgery, mean	0.74; P1=0.125
Latest follow-up, mean	0.42; P2=0.004, P3=0.002
Clinical symptoms of MMA, n=31	
Improvement	26
Disappearance	5
Deterioration	0
Complications, n=6	
Epileptic seizures	2
Cerebral hyper-perfusion syndrome	2
Intracranial rebleeding	2
Wound complications, n=2	
Skin necrosis	1
Skin maceration	1
Matsushima grade of synangiosis collaterals, n=31	
A	10
B	20
C	1

mRS, modified Rankin scale; MMA, moyamoya angiopathy; P1, admission *vs.* one month; P2, one month *vs.* latest follow-up; P3, admission *vs.* latest follow-up.

Table S3 Comparison of mRS scores in different time periods of moyamoya disease and subtypes

Target	mRS Score, mean ± standard deviation			z-Score, P value		
Variable	Admission	One month	Latest follow-up	P1	P2	P3
MMA	1.00±0.68	0.74±0.86	0.42±0.86	–1.54, 0.125	–2.89, 0.004*	–3.05, 0.002*
Ischemic	1.54±0.66	0.92±0.88	0.54±0.72	–3.87, 0.000*	–2.71, 0.007*	–4.18, 0.000*
Hemorrhagic	0.57±0.53	0.14±0.38	0	–1.73, 0.083	–1.00, 0.317	–2.00, 0.046*

*, statistical significance (P<0.05). mRS, modified Rankin scale; MMA, moyamoya angiopathy; Ischemic, ischemic moyamoya disease; Hemorrhagic, hemorrhagic moyamoya disease; P1, admission versus one month; P2, one month *vs.* latest follow-up; P3, admission *vs.* latest follow-up.

© Annals of Translational Medicine. All rights reserved.
https://dx.doi.org/10.21037/atm-22-5281

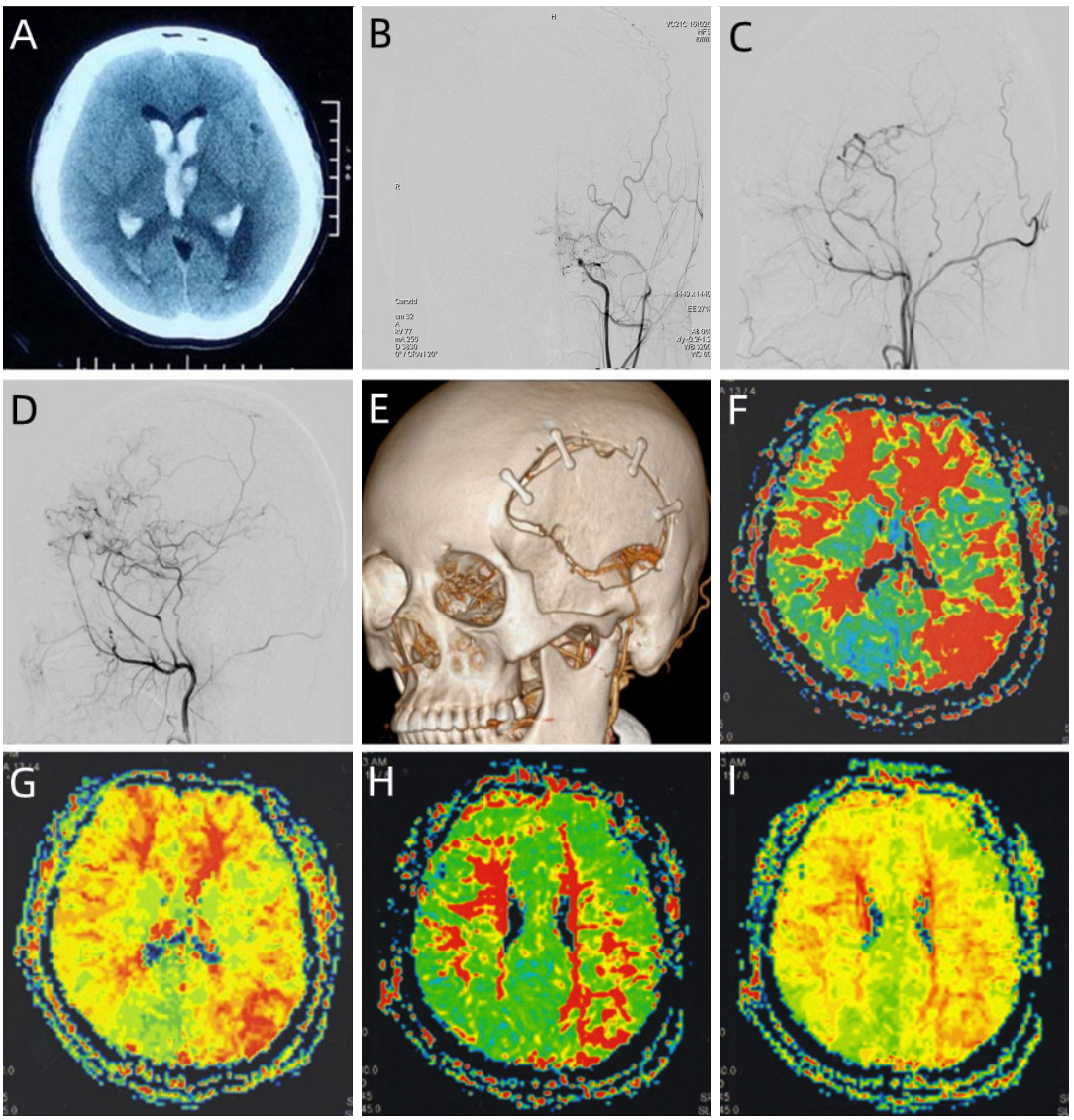

Figure S4 Preoperative and postoperative radiological findings of a 28-year-old woman. (A) Head computed tomography shows left thalamic hemorrhage broken into ventricles. (B) MMD Suzuki stage IV. (C,D) postoperative angiography shows a left STA frontal branch bypass. Long-term angiography shows extensive collateral anastomosis between STA and cerebral cortex, regarded as Matsushima grade A. (E) Postoperative 3D computed tomography scans of the skull. Note the cranial windows to prevent compression at the pedicle of TPFF for surgical revascularization. (F-H) MTT changes of MRP before and after surgery, and MTT of the left cerebral hemisphere is significantly shortened. (G-I) TTP changes of MRP before and after surgery, and TTP of the left cerebral hemisphere is significantly shortened too. MMD, moyamoya disease; STA, superficial temporal artery; TPFF, temporoparietal fascial flap; MRP, magnetic resonance perfusion; MTT, mean transit time; TTP, time to peak.

© Annals of Translational Medicine. All rights reserved.
https://dx.doi.org/10.21037/atm-22-5281

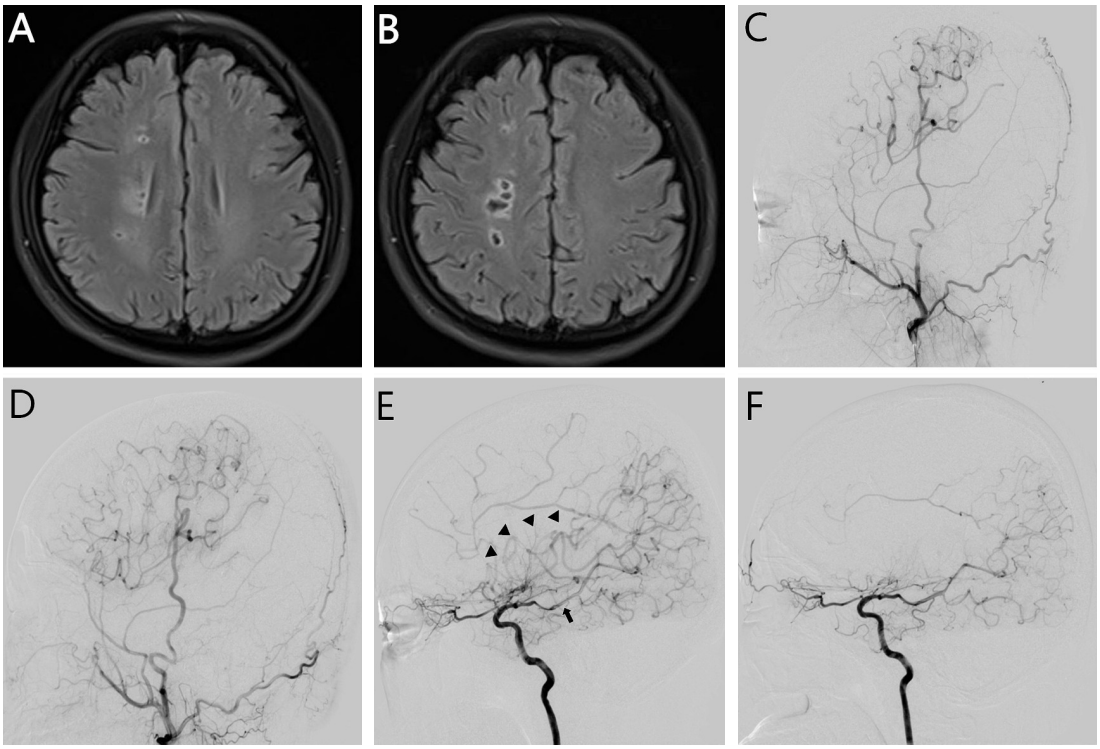

Figure S5 Preoperative and postoperative radiological findings of a 36-year-old woman. (A,B) Flare magnetic resonance imaging showing right frontal-parietal and periventricular infarction. (C,D) Postoperative angiography shows a right STA parietal branch bypass. Long-term angiography shows extensive collateral anastomosis between STA and cerebral cortex, regarded as Matsushima grade A. (E) Preoperative carotid angiography showed the formation of moyamoya vessels on the skull base (arrowheads), and anastomosis is formed between the posterior lateral choroidal artery (arrow) and pericallosal artery. (F) Long-term angiography showing the extensive disappearance of moyamoya vessels in the skull. STA, superficial temporal artery.

© Annals of Translational Medicine. All rights reserved.
https://dx.doi.org/10.21037/atm-22-5281

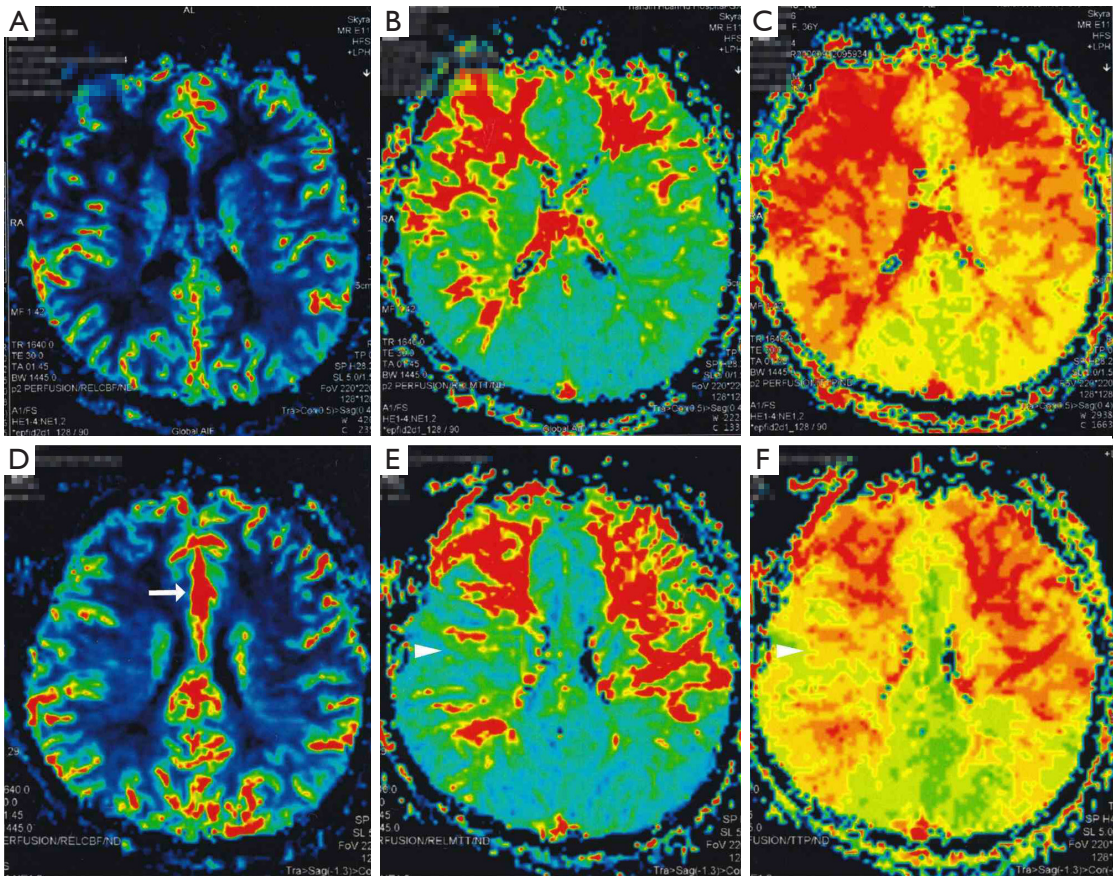

Figure S6 Preoperative, and long-term changes in MRP (A,D), TTP (B,E), and MTT (C,F) in a 36-year-old woman. CBF in the distribution of the anterior cerebral artery was increased (arrow), and TTP and MTT in the right frontal-parietal region were shortened (arrowhead). MRP, magnetic resonance perfusion; TTP, time to peak; MTT, mean transit time; CBF, cerebral blood flow.

© Annals of Translational Medicine. All rights reserved.
https://dx.doi.org/10.21037/atm-22-5281